

Hyperbolic Tiling on the Gyroid Membrane in Star Block Copolymers

Tomonari Dotera¹, Kenichi Hayashida^{2 3}, Junichi Matsuzawa⁴,
Atsushi Takano¹, & Yushu Matsushita^{1 5}

¹ Department of Physics, Kinki University, Higashi-Osaka 577-8502, Japan.

² Department of Applied Chemistry, Nagoya University, Nagoya 464-8603, Japan.

³ Present address: Organic Materials Research Lab, Toyota Central R&D Labs., Inc., Nagakute, Aichi 480-1192, Japan.

⁴ Department of Mathematics, Nara Women's University, Nara 630-8506, Japan.

⁵ Corresponding author.

Regular arrangements of atoms and molecules on spheres, cylinders, and flat planes are ubiquitous in various areas of material and biological sciences: *e.g.* fullerenes, carbon nanotubes, graphenes; icosahedral and helical capsids. Yet regular arrangement on saddle-shaped surfaces, referred to as hyperbolic tiling structure^{1–6}, has been discovered just for inorganic mesoporous materials⁷. Organic materials such as lipids, surfactants and copolymers are known to form cubic phases associated with periodic minimal (saddle-shaped) surfaces^{8–10}, however, decoration on the surfaces has not been found. Here we show a hyperbolic tiling structure obtained from an ABC star-shaped block copolymer composed of polyisoprene (I), polystyrene (S), and poly(2-vinylpyridine) (P). Transmission electron microscopy (TEM) and small-angle X-ray scattering (SAXS) demonstrate that the P component constructs two interpenetrating struts separated by a S and I gyroid membrane, and the tessellation of I spheroids on the membrane can be viewed as a hyperbolic Archimedean tiling on the Poincaré disk, or equivalently, the arrangement of angels in Escher’s Circle Limit IV. Combined with simulation data of hard spheres, the result suggests that hyperbolic tiling can be realised in biological membranes¹¹, or nanostructures of future plastic technologies¹².

Block copolymers are composed of two or more blocks of different polymer chains linked at junctions, acting as powerful agents to construct nanostructures¹². Not only spherical, cylindrical, and lamellar (flat-plane) phases, but also saddle-shaped surface structures associated with the gyroid (G) minimal surface called gyroid phases have been obtained from AB and ABC linear-type block copolymers^{13,14}. Recently, eigenvalue problems on periodic saddle-shaped surfaces such as photonic and electronic ones have attracted much attention^{15–17}. Moreover, in the case of ABC star-type block copolymers^{18–21}, our systematic investigation of ISP star-shaped polymers has shown novel morphologies: for instance, polygonal cylinders such as Archimedean and quasicrystalline tiling phases, and a zincblende structure^{22–25}. Gyroid phases for ABC star-type block copolymers, however, have not been found. Below we show evidence for a new kind of G-surface related structures, a hyperbolic tiling structure for a pure ABC star terpolymer I_{1.0}S_{1.8}P_{3.2}. The details of sample preparation and morphological observation are described in the last part of the paper and supplementary information.

A hyperbolic tiling is the hyperbolic analogue of a tiling on a plane; it is a tiling on a hyperbolic plane and is usually depicted on the Poincaré disk representing hyperbolic geometry¹: A household example is Escher’s enchanting series of artworks “Circle limit (Fig.S1).” More

than two decades ago, Charvolin and Sadoc pointed out that the Poincaré disk in Fig.1a tiled by $(\pi/2, \pi/4, \pi/6)$ -triangles is group-theoretically related to the G surface². The dodecagonal region within twelve thick curves in Fig.1a can be conformally mapped upon the G surface and cover a half area of the surface in a unit cell. A useful fact is that the symmetry operation of $Ia\bar{3}d$ is lifted to the orientation-preserving group action on Fig.1a. Indeed, the red and yellow circles in Fig.1a correspond to Wyckoff positions²⁶ of $Ia\bar{3}d$, $16a$ and $24d$, respectively; whose positions are geometrically monkey and horse saddle points¹ of the G surface, respectively (Fig.S2).

We propose a new Archimedean tiling ($3^3.4.3.4$) on the G surface (Figs.1b-d and Movie S1) obtained from green open circles in shaded triangles in Fig.1a. The set of integers $(n_1.n_2.n_3.\dots)$ denotes a tiling of a vertex-type in the way that n_1 -gon, n_2 -gon, and n_3 -gon, \dots , meet consecutively on each vertex, and superscripts are employed to abbreviate when possible. Each centre of shaded triangles made by one $16a$ and two $24d$ positions corresponds to a vertex of a ($3^3.4.3.4$) tiling (Fig.1b). Since the mapping preserves local connectivity, every vertex of ($3^3.4.3.4$) tiling has six neighbours and the same local environment. Thus, we call it Archimedean tiling even for hyperbolic geometry. In this sense, the tiling is a simple hyperbolic extension of the flat plane tessellation (3^6). The whole area is divided into alternating white and gray regions in Fig.1a, and then the inversion symmetry of $Ia\bar{3}d$ (No.230) is broken. This procedure enable us to find a curious coincidence between the tessellation of green circles in Fig.1a and that of angels (or devils) in Escher's Circle Limit IV (Fig.S1). Forty-eight vertex positions of the tiling in Figs.1c and 1d are generated by symmetry operations of space group $I\bar{4}3d$ (No.220), which is one of the cubic subgroups of $Ia\bar{3}d$, but not another subgroup $I4_1\bar{3}2$ (No.214) associated with the single-gyroid phase.

Furthermore, there exist a point and its symmetry equivalents on the G surface calculated by the Weierstrass-Enneper representation⁸ (Eq.S1) such that all edge lengths take the same value²⁷. The property of equidistance (0.259 in the unit of the lattice constant) is advantageous to entropic ordering, which principle prevails among many soft-matter systems. In fact, using Monte Carlo (MC) simulation, we found that 864 hard spheres (48 per unit cell) whose centres were confined on the G surface were self-organised into the angel ($3^3.4.3.4$) tiling as shown in Fig.1e. It exhibited an Alder entropy-driven first-order liquid-solid transition²⁸, when the radius of hard spheres was greater than about 0.118 in the unit of the lattice constant. To see the first-order transition, Fig.1f plots the movable probability

(acceptance ratio) of MC trial moves as a function of a hard-sphere radius. At each radius, 10^6 MC steps were performed. The plot indicates hysteresis curves depending on increasing and decreasing paths, and on random events. For the tiling configurations, we observed higher probability ensuring entropic stability of the ordered states. Periodic boundary conditions for x , y , and z directions were exerted, and in the green region spheres were fixed on angel regular sites that played a role of a solid interface. Without the solid region, we found random configurations frustrated with angel and devil tilings, which ended up with glassy states. This simulation result may hint why the hyperbolic tiling can be formed, and this is a physical reason why we adopt the tiling as a plausible structural candidate for the present polymeric system.

Based on the above mathematical and physical observations, we propose a structure model shown in Fig.1g and Movie S2, which turns out to be consistent with our present experimental results. We assume that the I domains are ellipsoidal shapes (prolate spheroids) with $r_a = r_b < r_c$ and $r_c/r_a = 1.3$, where r_α is the radius of the spheroid, and that the arrangement of centres of compact I domains is a hyperbolic Archimedean tiling ($3^3.4.3.4$) structure. The centre positions are $(0.576, 0.383, 0.554)$ and its symmetry equivalents. Major axes are set to be perpendicular to the G surface. Our choices are $r_a = 0.0859$ and $r_c = 0.112$. We assume that a three-dimensionally continuous but perforated S domain is represented by

$$|\sin kx \cos ky + \sin ky \cos kz + \sin kz \cos kx| < 0.678,$$

where $k = 2\pi/a$ and a denotes the lattice constant, and I domains are excluded. These I and S constitute a G membrane and contain the G surface as a neutral surface. These values of r_a , r_c , and 0.678 are determined so as to set the volume fractions I:S:P=1.0:1.8:3.2. Finally, P domains occupy remaining two separate spaces, which constitutes two gyroidal struts. The schematic picture of ISP polymers in Fig.1h displays how the polymers distribute in the structure. Junction points of three polymer blocks are on green circular lines where three components meet. Polymers densely fill the space, but not all polymers are illustrated for clarity.

With respect to experimental evidences, we first show TEM images and compare them with the model structure. Fig.2a shows a TEM image of the [111] projection for the $I_{1.0}S_{1.8}P_{3.2}$ sample stained with I_2 , which stains P component selectively. Black dots form a

honeycomb pattern corresponding to a straight path of the double-gyroid struts of P along [111] corresponding to hollow paths in Fig.1d. Fig.2b renders the simulation of the model. The relative contrast was represented by 0.3 for S and I, 1.0 for P in the case of I_2 . Not only black dots, but also bright separators in the midst of two dots are reproduced by the model structure. Furthermore, the lattice constant a is estimated from the relationship; $a = \sqrt{6}d/2$, where d denotes the centre-to-centre distance of the honeycomb pattern. The average value of d in Fig.2a gives a lattice constant of ~ 90 nm. See also supplemental Fig.S5 for the [001] projection, where we observed 4_1 and 4_3 screw axes of $Ia\bar{3}d$ or $I\bar{4}3d$. Many TEM images were taken in our TEM observation. A representative TEM image of the $I_{1.0}S_{1.8}P_{3.2}$ sample stained with I_2 are displayed in Fig.2c. The simulation reproduces hairpin curves and sequential dots in Fig.2d. Fig.2e shows a TEM image for a sample cut into ultrathin sections of 50 nm thickness and stained with OsO_4 and I_2 . The osmium tetroxide (OsO_4) stains the I component heavily. Clearly, I component constitute isolated domains and it appears that the shape is prolate. See supplemental Fig.S6 in detail. Fig.2f is the simulation for TEM stained OsO_4 . The relative contrast was represented by 0.1 for S, 0.3 for P, and 1.0 for I in the case of OsO_4 . We find that the arrangement of I domains is somehow regular but there are intermittent holes, and that the distance between I domains appears to be equal to or greater than 25 nm. These TEM results evidence the gyroid struts and isolated I domains embedded in the gyroid membrane.

Second, we show crystallographic data of the new structure which were obtained by microbeam X-ray scattering (SAXS) with an approximate beam size of $5\ \mu m \times 5\ \mu m$ (fwhm). Figs.3a-c show microbeam SAXS patterns of the $I_{1.0}S_{1.8}P_{3.2}$ sample from the [001], [011], and [111] directions. The magnitude q of the scattering spots are located at

$$\left(\frac{a}{2\pi}\right)q = \sqrt{6}, \sqrt{8}, \sqrt{14}, \sqrt{16}, \sqrt{20}, \sqrt{22}, \sqrt{24}, \dots,$$

where a is the lattice constant. This diffraction series is consistent with that for double-gyroid structures with $Ia\bar{3}d$ space group, and the lattice constant is calculated to be 103 nm from SAXS data in Fig.3a, which agrees with the value of about 90 nm estimated from the TEM images. To calculate scattering intensities, the scattering potential, which is proportional to electron densities for each component, is given by $f(\mathbf{r}) = 3.12, 3.40$, and 3.66, for I, S, and P, respectively, where $\mathbf{r} = (x, y, z)$. The scattering intensity is proportional to $|f_t(\mathbf{q})|^2$, where $f_t(\mathbf{q})$ is the Fourier transform of $f(\mathbf{r})$. To quantify, we calculate spherically

averaged intensities as a function of $q = (2\pi/a)\sqrt{h^2 + k^2 + l^2}$, where h , k , and l are scattering indexes. Overall calculated intensities of the model (Fig.3d) and the SAXS peaks are in good agreement: (1) Two prominent peaks $\sqrt{6}$ ($\{211\}$) and $\sqrt{8}$ ($\{220\}$) are strong as expected for the gyroid structure; (2) $\sqrt{22}$ ($\{332\}$) is the third strongest; (3) $\sqrt{20}$ ($\{420\}$) is weaker than $\sqrt{16}$ ($\{400\}$); (4) $\sqrt{26}$ ($\{431\}$) is visible. Contrary to the (3³.4.3.4) model, another tiling model (3⁶; 3⁸) described in supplementary information is inconsistent with (2)-(4). We note that the (3³.4.3.4) model is different in space-group symmetry, thus additional peaks ($\{310\}$ -type) may be observed. But the calculated intensity is too small to be detected in SAXS experiments.

Including the hyperbolic tiling structure, we made a phase diagram of ISP star polymers as shown in Fig.4. In the series of $I_{1.0}S_{1.8}P_X$ displayed by a red line, the P domains vary from the cylinders (Fig.4e, $0.8 \leq X \leq 2.9$) to the lamellae (Fig.4c, $4.3 \leq X \leq 11$) with increasing the volume ratio of the P component²⁹. In-between we have hyperbolic tiling on gyroid structures with $3.2 \leq X \leq 3.8$. See supplemental information. The shapes of the P domains are varied from cylinders to gyroid struts, to lamellae, and to matrix with increasing X . Although this morphological transition is quite analogous to that of AB-diblock copolymers, we should point out that the component forming gyroidal struts is a majority component in the new gyroid structure, while it is a minority one in diblock copolymers. In other words, the gyroid membrane is thinner than that of a linear-type polymer. We think that this ratio difference may be due to the effect of branched polymers.

In the series of $I_{1.0}S_{1.0}P_X$ displayed by a blue line, lamellae-in-lamella (Fig.4h) was found instead of cylinders-in-lamella³⁰. In this series, no gyroid structure but a disordered one was observed between them by careful inspection, although this was not mentioned in the reference. Interestingly, a Monte Carlo simulation study could not determine a definite structure in this window for $A_1B_1C_X$ star-shaped block copolymer systems as well¹⁹. The reason why the disordered phases were obtained is the following. If the I and S components are almost equal amounts, hierarchical lamellar domains (such as Fig.4h) are expected, however, it seems to be geometrically difficult to extend them over the G surface.

In conclusion, the hyperbolic Archimedean tiling (3³.4.3.4) on the G-surface was proposed, and its realisation with a lattice constant of 100 nm was verified in an ABC star-shaped block copolymer system. We found numerically that the tiling was self-organised even in a hard-sphere system, and thus our investigation opens up the possibility of regular arrangement

on saddle-shaped membranes in versatile soft materials.

METHODS

Sample Preparations. ABC Star-shaped block copolymer samples composed of polyisoprene (I), polystyrene (S) and poly(2-vinylpyridine) (P) were synthesized by anionic polymerizations as reported previously²². In supplemental information, we provide a table, which summarizes the volume ratios of the three components in two ISP star-shaped block polymer samples, used in this study together with their molecular weights and molecular weight distributions (MWDs).

Morphological Observations. Sample films were obtained by solvent-casting from 5% solutions of the ISP star polymer samples in THF for 2 days. The films were dried at room temperature for 12 h and annealed at 170 °C under a vacuum for 3 days.

For TEM observations, the films were cut into ultrathin sections having a thickness of 50 or 100 nm using an ultramicrotome (Reica Ultracut FCS), and they were observed on a transmission electron microscope (Hitachi, H-800). Microbeam SAXS measurements were performed using beamline BL40XU at SPring-8 facility (Hyogo, Japan). See supplemental information in detail.

Supplementary information and movies are available in the online version.

-
- ¹ Hilbert, D. & Cohn-Vossen, S., *Geometry and the Imagination*, (1932, American Mathematical Society; Reprint edition, 1999).
- ² Charvolin, J. & Sadoc, J. F., Periodic systems of frustrated fluid films and bicontinuous cubic structures in liquid crystals, *J. Physique*, **48**, 1559-1569 (1987).
- ³ Mackay, A. L. & Terrones, H., Diamond from graphite, *Nature*, **352**, 762 (1991).
- ⁴ Nesper, R. & Leoni, S., On tilings and patterns on hyperbolic surfaces and their relation to structural chemistry, *ChemPhysChem* **2**, 413-422 (2001).
- ⁵ Ramsden, S. J., Robins, V. & Hyde, S. T., Three-dimensional Euclidean nets from two-dimensional hyperbolic tilings: kaleidoscopic examples, *Acta Cryst. A* **65**, 81-108 (2009).
- ⁶ Modes, C. D. & Kamien, R., Hard disks on the hyperbolic plane, *Phys. Rev. Lett.* **99**, 235701 (2007).

- ⁷ Zou, X. *et al.* A mesoporous germanium oxide with crystalline pore walls and its chiral derivative, *Nature*, **437**, 716-719 (2005).
- ⁸ Schoen, A. H., Infinite periodic minimal surfaces without self-intersections, *NASA Technical Note*, TN D-5541 (1970).
- ⁹ Gózdż, W., & Hołyst, R., From the Plateau problem to periodic minimal surfaces of lipids, surfactants and diblock copolymers, *Macromol. Theory Simul.* **5**, 321-332 (1996).
- ¹⁰ Hyde, S. *et al.* *The Language of Shape* (Elsevier, Amsterdam, 1997).
- ¹¹ Baumgart, T., Hess, S. T., & Webb, W. W., Imaging coexisting fluid domains in biomembrane models coupling curvature and line tension, *Nature* **425**, 821 (2003).
- ¹² Ruzette, A.-V. & Leibler, L., Block copolymers in tomorrow's plastics, *Nature Mater.* **4**, 19-31 (2005).
- ¹³ Hajduk, D. A. *et al.* The gyroid: a new equilibrium morphology in weakly segregated diblock copolymers, *Macromolecules* **27**, 4063-4075 (1994).
- ¹⁴ Matsushita, Y., Suzuki, J. & Seki, M., Surfaces of tricontinuous structure formed by an ABC triblock copolymer in bulk, *Phys. B: Condens. Matter.* **248**, 238-242 (1998).
- ¹⁵ Maldovan, M. & Thomas, E. L., Diamond-structured photonic crystals. *Nature Mater.* **3**, 593-600 (2004).
- ¹⁶ Koshino, M. & Aoki, A., Electronic structure of an electron on the gyroid surface: A helical labyrinth, *Phys. Rev. B* **71**, 073405 (2005).
- ¹⁷ Fujita, N. & Terasaki, O., Band structure of the P, D, and G surfaces, *Phys. Rev. B* **72**, 085459 (2005).
- ¹⁸ Bohbot-Raviv, Y. & Wang, Z.-G., Discovering new ordered phases of block copolymers, *Phys. Rev. Lett.* **85**, 3428-3431 (2000).
- ¹⁹ Gemma, T., Hatano, A. & Dotera, T., Monte Carlo simulations of the morphology of ABC star polymers using the diagonal bond method, *Macromolecules* **35**, 3225-3237 (2002).
- ²⁰ Ueda, K., Dotera, T. & Gemma, T., Photonic band structure calculations of two-dimensional Archimedean tiling patterns, *Phys. Rev. B* **75**, 195122 (2007).
- ²¹ Matsushita, Y., Hayashida, K. & Takano, A. Jewelry box of morphologies with mesoscopic length scales - ABC star-shaped terpolymers, *Macromol. Rapid Commun.* in press.
- ²² Takano, A. *et al.* Observation of cylinder-based microphase-separated structures from ABC star-shaped terpolymers investigated by electron computerized tomography, *Macromolecules*

- 37**, 9941-9946 (2004).
- ²³ Takano, A. *et al.* A mesoscopic Archimedean tiling having a new complexity in an ABC star polymer, *J. Polym. Sci., Part B: Polym. Phys.* **43**, 2427-2432 (2005).
- ²⁴ Hayashida, K., Takano, A., Dotera, T. & Matsushita, Y., Polymeric quasicrystal: mesoscopic quasicrystalline tiling in ABC star polymers, *Phys. Rev. Lett.* **98**, 195502 (2007).
- ²⁵ Hayashida, K., Takano, A., Dotera, T. & Matsushita, Y., Giant zincblende structures formed by an ABC star-shaped terpolymer/homopolymer blend system, *Macromolecules* **41**, 6269-6271 (2008).
- ²⁶ Theo Hahn ed., *International Tables for Crystallography, Volume A: Space Group Symmetry, 5th ed. 2nd printing*, (Springer, New York, 2002).
- ²⁷ Dotera, T., & Matsuzawa, J. to be published in Kokyuroku, RIMS, Kyoto University.
- ²⁸ Alder, B. J. & Wainwright, T. E. Phase Transition for a Hard Sphere System, *J. Chem. Phys.* **27**, 1208-1209 (1957).
- ²⁹ Hayashida, K. *et al.* Hierarchical morphologies formed by ABC star-shaped terpolymers, *Macromolecules* **40**, 3695-3699 (2007).
- ³⁰ Takano, A. *et al.* Composition dependence of nanophase-separated structures formed by star-shaped terpolymers of the $A_{1.0}B_{1.0}C_X$ type, *J. Polym. Sci., Part B: Polym. Phys.* **45**, 2277-2283 (2007).

Acknowledgements We appreciate S.Arai and N.Sonoda for assistance with TEM experiments, D.Kawaguchi and S.S.B.Abdul Rahman for assistance with SAXS measurements, N.Ohta for Microbeam X-ray experiments under the Proposal No.2007B1088, and N.Fujita and M.Koiso for useful discussions. Finally, we are grateful to L.Leibler for helpful comments on the manuscript. This work was supported by a grant from PRESTO, JST, and Grant-in-Aid for Scientific Research on Priority Areas (No.18068008 & 20045006) from MEXT, Japan.

Author Contributions The experimental work was done by K.H., A.T. and Y.M. Theoretical analysis was provided by T.D. and J.M. The manuscript was written with substantial contributions from T.D. and K.H.

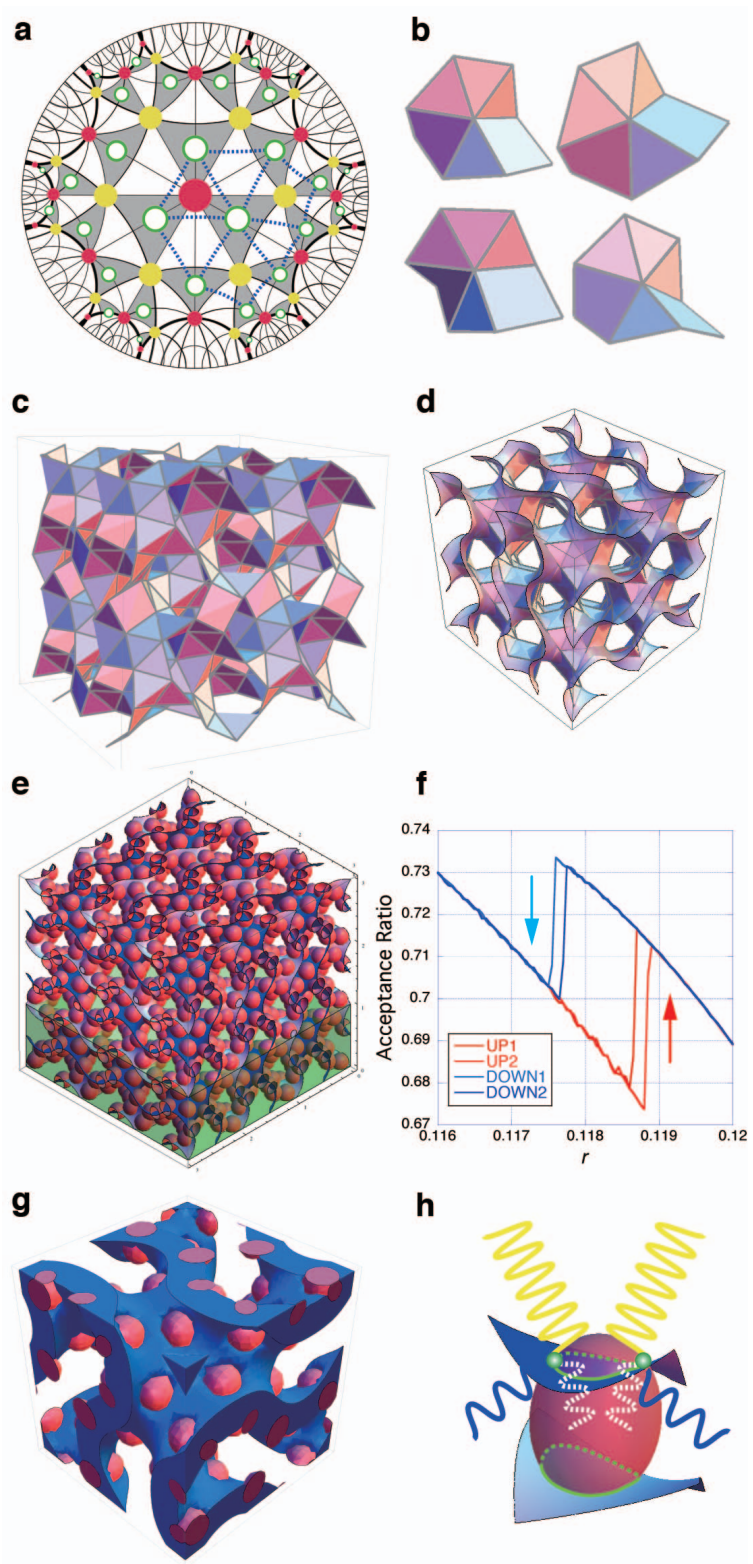


FIG. 1:

Fig.1: **a**, Poincaré disk tiled with $(\pi/2, \pi/4, \pi/6)$ -triangles (halves of white or shaded ones). The red and yellow circles correspond to Wyckoff positions of $Ia\bar{3}d$, $16a$ and $24d$, respectively. Green open circles in shaded triangles correspond to vertices of the $(3^3.4.3.4)$ tiling (blue dotted lines). **b**, $(3^3.4.3.4)$ vertex surrounded by six polygons in several views. One tetragon are almost a flat square, while the other equilateral tetragon is not. **c**, $(3^3.4.3.4)$ Archimedean tiling in a two-periodic cell. **d**, The same viewed from the [111] direction superimposed with the G surface. **e**, Self-assembly of hard spheres on the G surface in a three-periodic cell. **f**, Acceptance ratio of Monte Carlo trial moves as a function of a hard-sphere radius. **g**, Model structure (unit cell) of a hyperbolic tiling structure $(3^3.4.3.4)$ for $I_{1.0}S_{1.8}P_{3.2}$. The I component in red and the S component in blue are shown. Remaining transparent double channels are filled with the P component. **h**, Schematic pictures of two ISP star-shaped block copolymers around an I domain in Fig.1g: I (white), S (blue), P (yellow). Junction points of three polymer blocks displayed by green spheres are located on green circular lines where ISP meet.

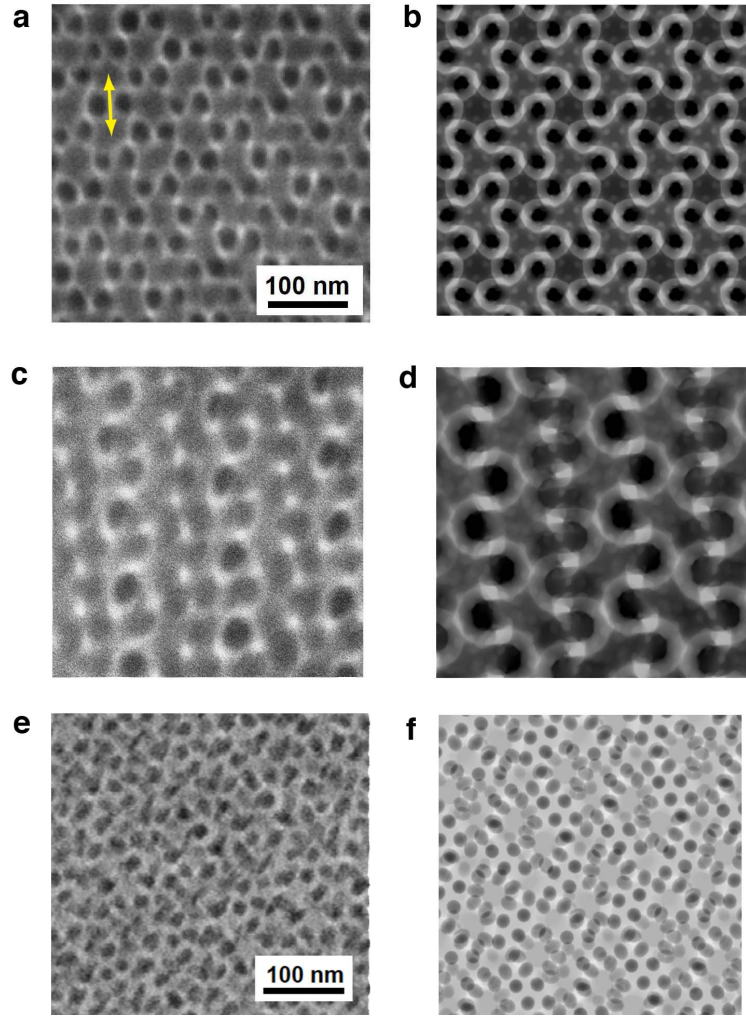


FIG. 2: **a**, TEM image of the [111] projection for the $I_{1.0}S_{1.8}P_{3.2}$ sample stained with I_2 ; The P component is seen in black. The thickness is 50 nm. **b**, TEM simulation perpendicular to [111] for $(3^3.4.3.4)$ model. The thickness is $0.6a$, where a is the lattice constant. The honeycomb pattern of black dots is reproduced. **c**, TEM image of the same sample as (a). The thickness is 100 nm. **d**, TEM simulation perpendicular to [5,6,13]. The thickness is $0.8a$. **e**, TEM image of the same sample stained with OsO_4 and I_2 . The thickness is 50 nm. **f**, TEM simulations stained with OsO_4 perpendicular to [122] for $(3^3.4.3.4)$ model. The thickness is $0.45a$.

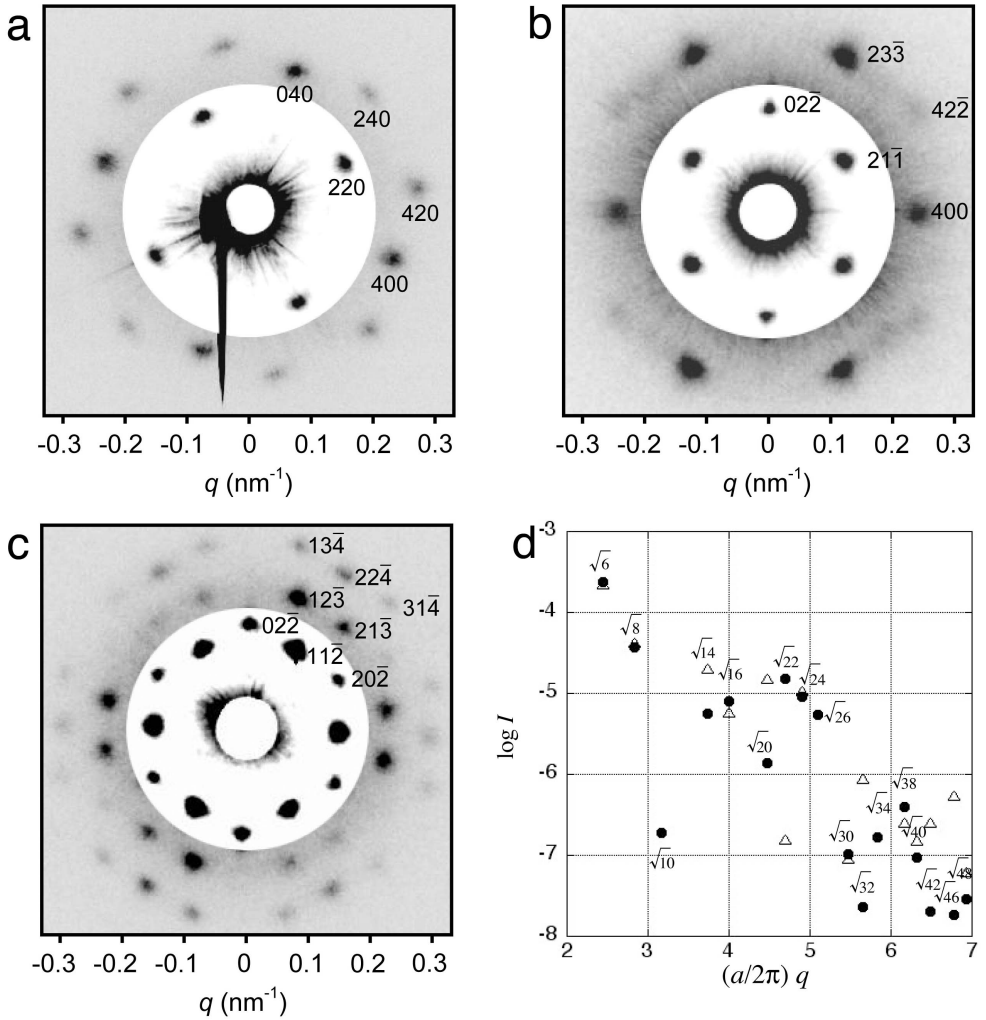


FIG. 3: Microbeam SAXS patterns of the $I_{1.0}S_{1.8}P_{3.2}$ sample from **a**, [001], **b**, [011], and **c**, [111] directions. The intensities of the outer scatterings are scaled up. **d**, Plot of calculated intensity for two hyperbolic tiling models. ●: $(3^3 \cdot 4 \cdot 3 \cdot 4)$, △: $(3^6; 3^8)$. Common logarithms $\log I$ as a function of $(a/2\pi)q$ is plotted, where I is the spherically averaged intensity of I_{hkl} divided by I_{000} .

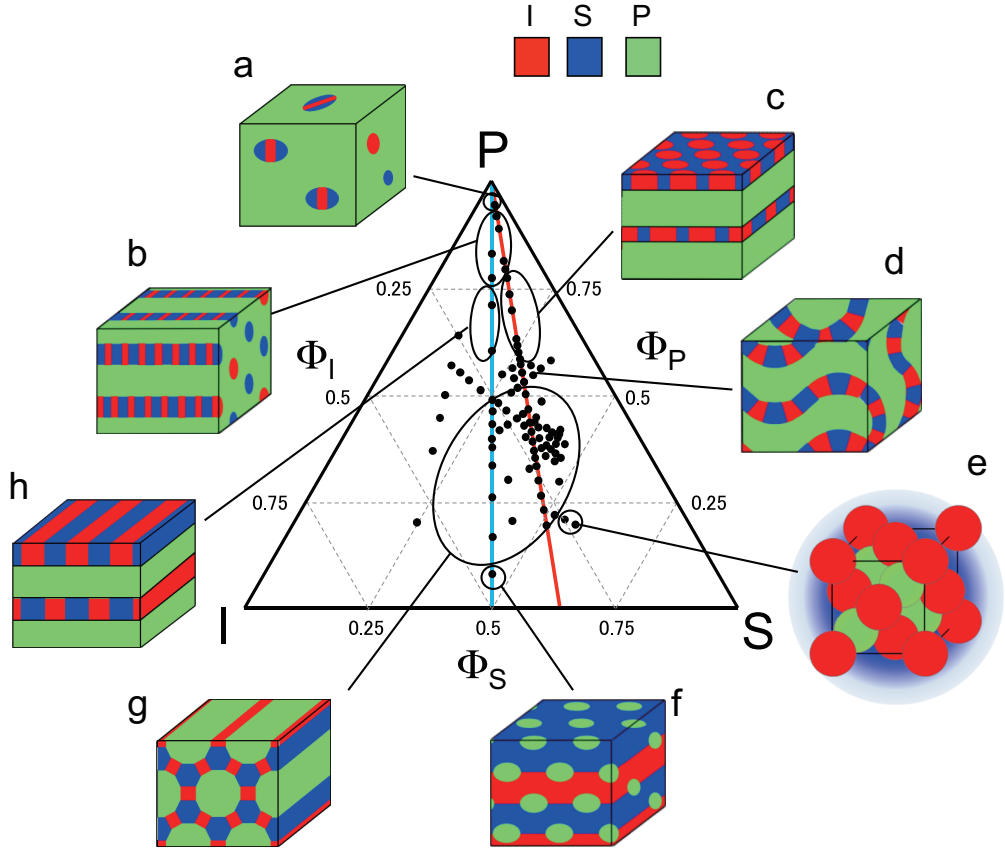


FIG. 4: Morphology of the ISP star-shaped block copolymer system. **a**, Lamellae-in-sphere. **b**, Lamellae-in-cylinder. **c**, Cylinders-in-lamella. **d**, Hyperbolic tiling-on-gyroid membrane. **e**, Polygonal cylinder; e.g. (4.6.12) Archimedean tiling pattern shown in the figure. **f**, Zincblende. **g**, Spheres+lamella. **h**, Lamellae-in-lamella. Red and blue lines indicate $I_{1.0}S_{1.8}P_X$ and $I_{1.0}S_{1.0}P_X$ series, respectively.